

Planar dicyclic B₆S₆, B₆S₆ –, and B₆S₆ 2– clusters: Boron sulfide analogues of naphthalene

Da-Zhi Li, Hui Bai, Ting Ou, Qiang Chen, Hua-Jin Zhai, and Si-Dian Li

Citation: *The Journal of Chemical Physics* **142**, 014302 (2015); doi: 10.1063/1.4904289

View online: <http://dx.doi.org/10.1063/1.4904289>

View Table of Contents: <http://scitation.aip.org/content/aip/journal/jcp/142/1?ver=pdfcov>

Published by the **AIP Publishing**

Articles you may be interested in

[A first-principles study on the B₅O₅ +/0 and B₅O₅ – clusters: The boron oxide analogs of C₆H₅ +/0 and CH₃Cl](#)

J. Chem. Phys. **143**, 064303 (2015); 10.1063/1.4928282

[Photoelectron spectroscopy of B₄O₄ –: Dual 3c-4e \$\pi\$ hyperbonds and rhombic 4c-4e \$\sigma\$ -bond in boron oxide clusters](#)

J. Chem. Phys. **142**, 134305 (2015); 10.1063/1.4916386

[Benzene analogues of \(quasi-\)planar M@B_nH_n compounds \(M = V–, Cr, Mn+\): A theoretical investigation](#)

J. Chem. Phys. **139**, 174310 (2013); 10.1063/1.4827517

[Perfectly planar boronyl boroxine D_{3h} B₆O₆: A boron oxide analog of boroxine and benzene](#)

J. Chem. Phys. **138**, 244304 (2013); 10.1063/1.4811330

[First principle structural determination of \(B₂O₃\)_n \(n = 1–6\) clusters: From planar to cage](#)

J. Chem. Phys. **138**, 094312 (2013); 10.1063/1.4793707



NEW Special Topic Sections

NOW ONLINE
Lithium Niobate Properties and Applications:
Reviews of Emerging Trends

AIP | Applied Physics
Reviews

Planar dicyclic B_6S_6 , $B_6S_6^-$, and $B_6S_6^{2-}$ clusters: Boron sulfide analogues of naphthalene

Da-Zhi Li,¹ Hui Bai,² Ting Ou,² Qiang Chen,² Hua-Jin Zhai,^{2,3,a)} and Si-Dian Li^{2,a)}

¹Department of Chemistry and Chemical Engineering, Binzhou University, Binzhou 256603, Shandong, People's Republic of China

²Nanocluster Laboratory, Institute of Molecular Science, Shanxi University, Taiyuan 030006, Shanxi, People's Republic of China

³State Key Laboratory of Quantum Optics and Quantum Optics Devices, Shanxi University, Taiyuan 030006, Shanxi, People's Republic of China

(Received 10 October 2014; accepted 1 December 2014; published online 5 January 2015)

Inorganic analogues of hydrocarbons or polycyclic aromatic hydrocarbons (PAHs) are of current interest in chemistry. Based upon global structural searches and B3LYP and CCSD(T) calculations, we present herein the perfectly planar dicyclic boron sulfide clusters: D_{2h} B_6S_6 (**1**, 1A_g), D_{2h} $B_6S_6^-$ (**2**, $^2B_{3u}$), and D_{2h} $B_6S_6^{2-}$ (**3**, 1A_g). These are the global minima of the systems, being at least 0.73, 0.81, and 0.53 eV lower in energy, respectively, than their alternative isomers at the CCSD(T) level. The D_{2h} structures feature twin B_3S_2 five-membered rings, which are fused together via a B_2 unit and terminated by two BS groups. Bonding analyses show that the closed-shell $B_6S_6^{2-}$ (**3**) cluster possesses 10 delocalized π electrons, closely analogous to the bonding pattern of the aromatic naphthalene $C_{10}H_8$. The $B_6S_6^-$ (**2**) and B_6S_6 (**1**) species are readily obtained upon removal of one or two π electrons from $B_6S_6^{2-}$ (**3**). The results build a new analogous relationship between boron sulfide clusters and their PAH counterparts. The $B_6S_6^-$ (**2**) monoanion and $B_6S_6^{2-}$ (**3**) dianion can be effectively stabilized in neutral LiB_6S_6 and $Li_2B_6S_6$ salts, respectively. © 2015 AIP Publishing LLC. [<http://dx.doi.org/10.1063/1.4904289>]

I. INTRODUCTION

As a prototypical electron-deficient element in the periodic table, boron has interesting chemical bonding properties. Boron clusters and boron-containing clusters^{1–13} are unique systems to address the structural diversity and bonding nature of boron at the molecular level. A number of recent studies show that there exist analogous relationships between boron-based clusters and the planar hydrocarbons, including polycyclic aromatic hydrocarbons (PAHs). For example, the D_{2h} B_4H_2 , C_{2h} B_8H_2 , and C_{2h} $B_{12}H_2$ clusters² are boron hydride analogues of the conjugated ethylene D_{2h} C_2H_4 , 1,3-butadiene C_{2h} C_4H_6 , and 1,3,5-hexatriene C_{2h} C_6H_8 , respectively. In terms of the nature of bonding, boron and boron-containing clusters are found to possess aromaticity and antiaromaticity according to the Hückel rules, akin to the hydrocarbon molecules. Notably, B_8^{2-} and B_9^- ,³ B_{10} , B_{11}^- , and B_{12} ,⁴ and B_{13}^+ as well⁵ all possess 6π electrons and can be viewed as inorganic analogues of benzene. The dianion B_{16}^{2-} cluster with 10π electrons is an all-boron analogue of naphthalene,¹ and B_{22}^- and B_{23}^- with seven delocalized π canonical molecular orbitals (CMOs) are all-boron analogues of anthracene and phenanthrene, respectively.⁶

Boronyl (BO) has emerged as a robust inorganic ligand during the past decade, from gas-phase clusters to synthetic compounds, where the BO triple bond dominates the structure and bonding of the systems, like the CN and CO ligands.

In a recent paper,¹¹ we presented a theoretical study on a unique boron oxide B_6O_6 cluster, which was predicted to be boronyl boroxine, D_{3h} $B_3O_3(BO)_3$, a new member of the “inorganic benzene” family. Similar to benzene, D_{3h} $B_3O_3X_3$ ($X = BO, H$) can be used as a ligand to form transition metal complexes, such as the sandwich-type D_{3d} $(B_3O_3X_3)_2Cr$,¹¹ D_{3d} $(B_3O_3X_3)_2V$,¹² and the perfectly planar $(B_3O_3H_3)_nM^+$ ($n = 1, 2; M = Cu, Ag, Au$) complexes.¹³ Given the close similarity between S and O in valence electron configurations, boron sulfide clusters may possess similar geometries and electronic structure with their corresponding boron oxides. However, in comparison with boron oxides, boron sulfide clusters have received rather limited attention in the literature, and the current understanding of the structural principles and bonding nature of the electron-deficient boron sulfide clusters remains inadequate.

Gas-phase mass spectroscopic studies about 30 years ago confirmed the existence of a wide range of boron sulfide cations, suggesting that BS_2^+ , $B_2S_2^+$, and $B_2S_3^+$ are the most important precursor ions to form the high molecular weight boron sulfide clusters.^{14–18} Two *ab initio* calculations on the BS diatomic species^{19,20} presented very different excitation energies (3.83 versus 2.47 eV) for transition from the ground state $BS^2\Sigma^+$ to the first excited state $BS^2\Pi$, with both values being significantly larger than the experimental term value (1.99 eV).²¹ Linear BS_2 neutral cluster was observed using the laser-induced fluorescence technique.^{22,23} Our group investigated very recently a series of simple boron sulfide clusters: BS, BS_2^- , $B(BS)_2^-$, $B(BS)_3^-$,²⁴ and $B(BS)_4^-$.²⁵ These boron sulfides were shown to possess similar geometric

a) Authors to whom correspondence should be addressed. Electronic addresses: hj.zhai@sxu.edu.cn and lisidian@sxu.edu.cn

structures with their oxide counterparts: BO, BO_2^- , $\text{B}(\text{BO})_2^-$, $\text{B}(\text{BO})_3^-$,²⁶ and $\text{B}(\text{BO})_4^-$.²⁵ It was revealed that boron-rich boron sulfide clusters favor the formation of the $\text{B} \equiv \text{S}$ groups, which basically serve as σ radicals and govern the global-minimum structures of the clusters.

Here, we report a systematic computational study on the structures and chemical bonding of the $\text{B}_6\text{S}_6^{0/-/2-}$ (**1–3**) clusters. The work involves global-minimum searches, density-functional theory (DFT) and coupled-cluster theory (CCSD(T)) calculations, and chemical bonding analyses. The global-minimum D_{2h} $\text{B}_6\text{S}_6^{0/-/2-}$ (**1–3**) structures exhibit twin, fused B_3S_2 five-membered rings with an elongated shape. A proposal is put forward that $\text{B}_6\text{S}_6^{0/-/2-}$ are inorganic analogues of naphthalene (C_{10}H_8). In particular, the five delocalized π CMOs in $\text{B}_6\text{S}_6^{2-}$ (**3**) show one-to-one correspondence to those in naphthalene, as revealed from the CMO analysis and the adaptive natural density partitioning (AdNDP).²⁷ The current work extends the boron sulfide chemistry, suggesting that a variety of new boron sulfide clusters may be designed on the basis of their analogy to PAHs. To assess the viability of B_6S_6^- (**2**) and $\text{B}_6\text{S}_6^{2-}$ (**3**) as potential building blocks for cluster assembled nanomaterials, we explored their salt complexes: LiB_6S_6 (**4**) and $\text{Li}_2\text{B}_6\text{S}_6$ (**5–7**). In such complexes, the B_6S_6^- or $\text{B}_6\text{S}_6^{2-}$ clusters are stabilized by one or two Li^+ counter cations, and their structural and chemical integrity are well maintained.

II. COMPUTATIONAL PROCEDURES

Global-minimum searches for B_6S_6 were conducted using the Gradient Embedded Genetic Algorithm (GEGA),^{28,29} Coalescence Kick (CK),^{30,31} and Basin Hopping (BH)³² algorithms, aided with extensive manual structural constructions. Further structural optimizations and frequency analysis were carried out for the low-lying isomers using the hybrid B3LYP method^{33,34} with the basis set of 6-311+G(d,p), as implemented in the Gaussian 03 program.³⁵ The top structures identified for B_6S_6 were used as the initial structures for B_6S_6^- and $\text{B}_6\text{S}_6^{2-}$ during their structural searches. To check for consistency, the relative energies were also calculated using the PBE0 functional with symmetry constraints.³⁶ Furthermore, the relative energies were refined for the low-lying isomers using the CCSD(T) method^{37–39} at the B3LYP geometries. AdNDP,²⁷ in combination with CMO analysis, was used to analyze the chemical bonding. The natural bond orbital (NBO) 5.0 program⁴⁰ was used to calculate the natural atomic charges. The adiabatic and vertical detachment energies (ADE and VDE) of B_6S_6^- were calculated using the time-dependent DFT (TD-DFT) method.^{41,42}

III. RESULTS

The global-minimum structure of B_6S_6 neutral, (**1**, D_{2h} , 1A_g), is shown in Fig. 1, along with those of D_{2h} B_6S_6^- (**2**, $^2B_{3u}$) and D_{2h} $\text{B}_6\text{S}_6^{2-}$ (**3**, 1A_g). Alternative optimized low-lying structures of $\text{B}_6\text{S}_6^{0/-/2-}$ at the B3LYP/6-311+G(d,p) level are depicted in the supplementary material (Figs. S1–S3),⁴³ where their relative energies at the B3LYP/6-311+G(d,p),

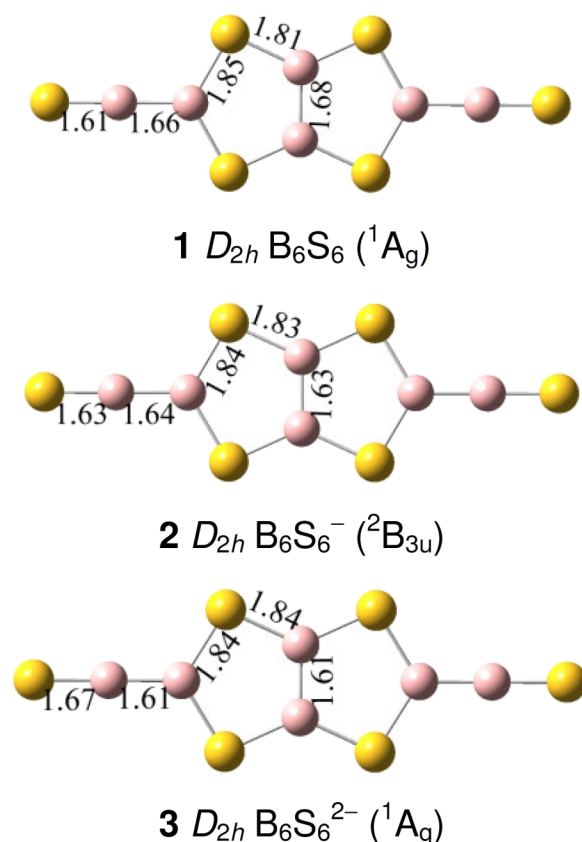


FIG. 1. Global-minimum D_{2h} structures of B_6S_6 (**1**, 1A_g), B_6S_6^- (**2**, $^2B_{3u}$), and $\text{B}_6\text{S}_6^{2-}$ (**3**, 1A_g) at the B3LYP/6-311+G(d,p) level. Selected bond distances are labeled in angstroms. Yellow color represents S atoms.

PBE0/6-311+G(d,p), and single-point CCSD(T)//B3LYP/6-311+G(d,p) levels are documented as well.

As shown in Figs. 1 and S1,⁴³ the B_6S_6 neutral cluster adopts a perfectly planar dicyclic **1** (D_{2h} , 1A_g) global-minimum structure. It possesses twin B_3S_2 five-membered rings as the core, with two BS units attached terminally. The overall shape is elongated. The highly symmetric circular B_6S_6 (D_{3h} , $^1A_1'$) structure is a low-lying isomer for the system (Fig. S1),⁴³ which lies 0.56 and 0.73 eV above the global minimum at the B3LYP and CCSD(T) levels, respectively. Note that the D_{3h} ($^1A_1'$) structure is the global minimum for the isovalent B_6O_6 cluster, for which the dicyclic D_{2h} (1A_g) isomer is 1.32 eV higher at the CCSD(T)//B3LYP/6-311+G(d,p) level.¹¹ Thus, the energetics for isomers alter markedly for the B—S versus B—O clusters.

Alternative B_6S_6 isomers are at least 0.4 eV above **1** (D_{2h} , 1A_g), making the latter the well-defined global minimum on the potential energy surface. Interestingly, all isomeric B_6S_6 structures (Fig. S1)⁴³ contain four-, five-, or six-membered B—S rings, with additional BS or BS_2 units attached terminally. A similar set of structures are located for B_6S_6^- and $\text{B}_6\text{S}_6^{2-}$ (Figs. S2 and S3).⁴³ The planar dicyclic **2** (D_{2h} , $^2B_{3u}$) and **3** (D_{2h} , 1A_g) structures are the global minima for B_6S_6^- and $\text{B}_6\text{S}_6^{2-}$, respectively (Fig. 1).

Selected bond distances are labeled for the global-minimum structures **1–3** (Fig. 1). The B—S bond distances of the terminal BS group in D_{2h} B_6S_6 (**1**, 1A_g), D_{2h} B_6S_6^- (**2**, $^2B_{3u}$), and D_{2h} $\text{B}_6\text{S}_6^{2-}$ (**3**, 1A_g) vary slightly, which are 1.61,

1.63, and 1.67 Å, respectively. These are typical B≡S triple bonds, being remarkably similar to those in B(BS)₂[−] and B(BS)₃[−],²⁴ B(BS)₄[−],²⁵ and B₂(BS)₆^{0/−}.⁴⁴ The calculated B—S bond distances within the dicyclic B₃S₂ rings (1.81–1.85 Å) should be roughly viewed as, or slightly stronger than, single bonds. For example, the corresponding B—S distances in **3** are 1.84 Å with an effective bond order of 1.19 (Table SI),⁴³ which is due to the existence of delocalized electrons in the B₃S₂ rings. All B—B bond distances in **1–3** (1.61–1.68 Å) are classified approximately as single bonds.

IV. DISCUSSION

A. Planar dicyclic D_{2h} B₆S₆^{2−} cluster: A boron sulfide analogue of naphthalene

The B₆S₆, B₆S₆[−], and B₆S₆^{2−} clusters adopt similar D_{2h} global-minimum structures: **1** (¹A_g), **2** (²B_{3u}), and **3** (¹A_g). The structures exhibit twin B₃S₂ five-membered rings as the core with two terminal BS groups. Their elongated overall shape is reminiscent of the naphthalene molecule (C₁₀H₈), one of the simplest PAHs. The CMO analyses immediately reveal that the delocalized π bonding pattern in **1–3** is similar to that in naphthalene (Fig. S4).⁴³ To be specific, the five delocalized π CMOs in B₆S₆^{2−} (**3**, ¹A_g) are basically eight-center two-electron (8c-2e) in nature and fully occupied with 10π electrons, showing one-to-one correspondence to those in naphthalene, except that the energy order of the top two CMOs reverses. The B₆S₆[−] (**2**, ²B_{3u}) and B₆S₆ (**1**, ¹A_g) species may be reached from B₆S₆^{2−} (**3**, ¹A_g) by removing one and two valence electrons from its highest occupied molecular orbital (HOMO). Based on the above analysis, the planar dicyclic B₆S₆^{2−} (**3**, ¹A_g) cluster is a close inorganic analogue of naphthalene, as the circular D_{3h} B₆O₆ cluster is an inorganic benzene or boroxine.¹¹ Inorganic analogues of naphthalene are rare in the literature. In a prior study, we reported a D_{2h} B₁₆^{2−} (¹A_g) cluster,¹ which also possesses an elongated shape with 10π electrons, akin to naphthalene.

To understand the nature of bonding in **1–3** in further detail, we performed the AdNDP²⁷ analysis for D_{2h} B₆S₆^{2−} (**3**). As an extension of the NBO analysis, AdNDP represents

the electronic structure of a molecular system in terms of n -center two-electron (nc -2e) bonds, where the values of n range from one to the total number of atoms in the system. AdNDP thus recovers not only the Lewis bonding elements (lone pairs and 2c-2e bonds), but also the delocalized nc -2e bonds. According to the AdNDP results (Fig. 2), of the 56 valence electrons in B₆S₆^{2−} (**3**), the σ framework involves 13 2c-2e bonds (plus the six S 3s lone-pairs; not shown): two terminal B—S σ bonds, three B—B σ bonds, and eight B—S σ bonds within the twin five-membered rings. This leaves nine bonds for the π framework, including four terminal 2c-2e π bonds for the two BS groups (first row; Fig. 2).

The remaining five π bonds are all 8c-2e in nature, being delocalized over the twin five-membered rings (third row; Fig. 2). It is these five 8c-2e π bonds that are responsible for the global delocalized bonding in B₆S₆^{2−} (**3**), which also define their close analogy to naphthalene. Among the corresponding delocalized π CMOs in B₆S₆^{2−} (**3**) (Fig. S4),⁴³ HOMO-1, HOMO-3, HOMO-11, and HOMO-12 are mainly derived from the bridging S atoms. The HOMO is largely based on the three B₂ units, but also has discernible contribution from the terminal S atoms; the latter is more clearly seen from the NBO charge distributions (**3** versus **1**; Table SI).⁴³

Note that all occupation numbers (ONs) in the AdNDP results are very close to the ideal value of 2.00 |e|, suggesting that the B—B and B—S bonding, both localized and delocalized, are well-defined. Indeed, the 17 2c-2e bonds (rows 1 and 2; Fig. 2) perfectly recover the B≡S, B—B, and B—S assignments, which are in line with their bond distances (Sec. III).

B. Comparison of the structures of sulfide and oxide clusters: D_{2h} B₆S₆ versus D_{3h} B₆O₆

B₆S₆ is isovalent to B₆O₆.¹¹ Both clusters are perfectly planar. However, their global-minimum structures differ markedly. B₆S₆ possesses the dicyclic D_{2h} structure with twin B₃S₂ five-membered rings (Fig. 1), which is 0.73 eV more stable than the monocyclic D_{3h} isomer at the CCSD(T) level.

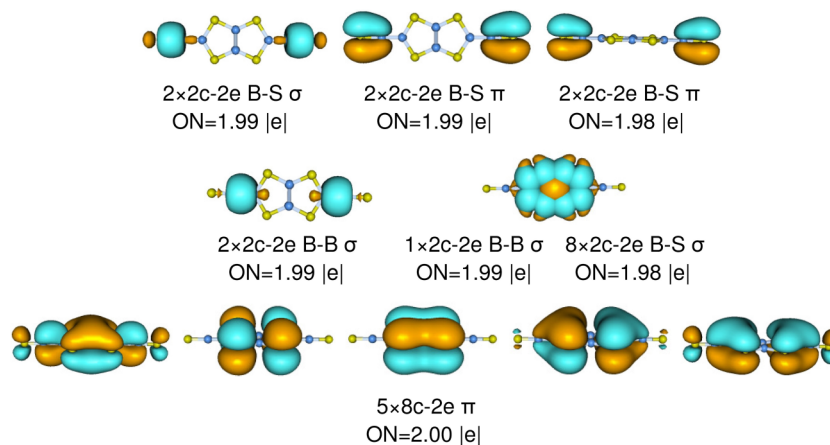


FIG. 2. AdNDP bonding pattern of D_{2h} B₆S₆^{2−} (**3**, ¹A_g). The occupation numbers (ONs) are shown.

In contrast, B_6O_6 is an analogue of benzene or boroxine,¹¹ which adapts the highly symmetric, monocyclic D_{3h} global minimum with a B_3O_3 six-membered ring, with the dicyclic D_{2h} structure being 1.32 eV higher in energy at the same level. It is thus of critical importance to understand the sharp difference between B_6S_6 and B_6O_6 in terms of structures and energetics. We believe two factors may hold the key to address this question.

First, the polar nature of B—O versus B—S interactions determines the intramolecular Coulomb repulsion in the systems. The difference of electronegativity between B and S is ~ 0.5 (Pauling scale) and that between B and O is ~ 1.4 . Thus, the B—S bond should be more covalent, whereas the B—O bond is rather polar. Indeed, the NBO charges in both the dicyclic D_{2h} and monocyclic D_{3h} structures of B_6S_6 are practically neutral for B and S in the rings. However, in both structures of B_6O_6 , there are substantial charge transfers from B to O within the rings (B +0.8 |e| versus O -0.8|e|; B3LYP data). Consequently, the B—O clusters tend to have more terminal BO groups in order to release and minimize the intramolecular Coulomb repulsion, and the monocyclic D_{3h} structure is its favorite choice. In particular, the Coulomb repulsion is anticipated to be severe in the D_{2h} B_6O_6 structure, which makes it energetically unfavorable. A second consequence is that B_6S_6 appears to be more aromatic than B_6O_6 . The calculated nucleus-independent chemical shift (NICS) values for D_{2h} B_6S_6 (**1**) at the pentagon center are $NICS(0) = -5.0$ ppm and $NICS_{zz}(1) = -13.7$ ppm at the B3LYP level, as compared to those for naphthalene at the hexagon center: $NICS(0) = -7.2$ ppm and $NICS_{zz}(1) = -28.3$ ppm. In contrast, the inorganic benzene D_{3h} B_6O_6 is barely aromatic with $NICS_{zz}(1) = -2.8$ ppm at the same level, which is significantly smaller than that for benzene with $NICS_{zz}(1) = -29.7$ ppm.¹¹

Second, for B_6S_6 , the Coulomb repulsion is no longer an issue and the appropriate size of BS rings becomes critical. For the D_{3h} B_6S_6 structure, the six-membered B_3S_3 ring has a diameter of ~ 3.6 Å, which is probably too large to form an effective π -system. For comparison, the diameter of the B_3O_3 ring in D_{3h} B_6O_6 is ~ 2.7 Å,¹¹ very close to that in benzene (~ 2.8 Å). On the other hand, the elongated twin B_3S_2 rings in **1–3** can support four or five delocalized π CMOs (Fig. S4),⁴³ which help stabilize the structures.

C. Growth pattern of the $B_{2n}S_{2n}$ ($n = 1–4$) series: B_2S_2 as possible structural unit

As shown in Fig. 3 and Fig. S5,⁴³ the linear B_2S_2 ($D_{\infty h}$, ${}^1\Sigma_g$) cluster with the bond distances of $r_{B=S} = 1.61$ Å and $r_{B-B} = 1.62$ Å is the ground state, which lies 2.12 and 1.78 eV lower than the second isomer D_{2h} B_2S_2 at the B3LYP and CCSD(T)//B3LYP levels, respectively. Other optimized structures are even higher in energy (by at least 2.58 eV at B3LYP level). Note that the linear B_2S_2 cluster is similar to its isovalent B_2O_2 counterpart⁴⁵ in geometry, although the B—X bond distances in B_2X_2 ($X = O, S$) increase substantially from $r_{B=O} \approx 1.20$ Å in the oxide^{11,25,45} to $r_{B=S} = 1.61$ Å in the sulfide^{20,24,25} due to the different atomic sizes of S versus O. The calculated energy gap for B_2S_2 between the HOMO and the lowest unoccupied molecular orbital (LUMO)

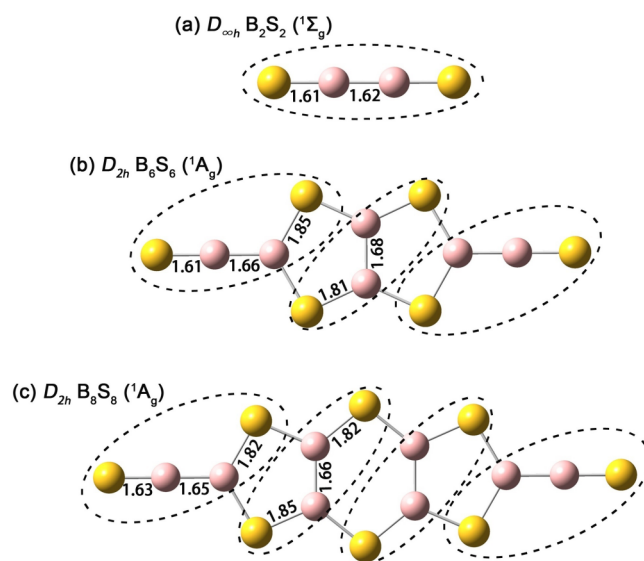


FIG. 3. Comparison of the optimized structures of B_2S_2 , B_6S_6 (**1**), and B_8S_8 neutral clusters at the B3LYP/6-311+G(d,p) level. Selected bond distances are labeled in angstroms. Yellow color represents S atoms.

is 5.14 eV (Table SI),⁴³ well supporting its high electronic stability.

Figure 3 depicts the optimized structures of the $B_{2n}S_{2n}$ ($n = 1, 3, 4$) series at the B3LYP level. The structural evolution hints that the linear B_2S_2 cluster may serve as a structural unit for boron sulfides. One can compare the ground-state geometries of B_2S_2 and B_6S_6 . In D_{2h} B_6S_6 (**1**, 1A_g), typical bond distances are $r_{B\equiv S_t} = 1.61$ Å, $r_{B-B} = 1.66–1.68$ Å, and $r_{B-S_b} = 1.81–1.85$ Å, where S_t and S_b stand for the terminal and bridging S atoms, respectively. When combining two B_2S_2 units for a B_3S_2 five-membered ring, one terminal S from each B_2S_2 is transformed to a bridging S, turning two terminal $B\equiv S$ bonds into four bridging B—S bonds. In the meantime, two S 3p lone-pairs are generated, which facilitate further π delocalization within the ring. By repeating this process, one can generate D_{2h} B_6S_6 (1A_g) and D_{2h} B_8S_8 (1A_g) (Fig. 3), where the former is the global minimum of the B_6S_6 system. The formation energy can be calculated using the equation: $3B_2S_2$ ($D_{\infty h}$, ${}^1\Sigma_g$) = B_6S_6 (D_{2h} , 1A_g). The formation energy thus evaluated is -70.2 kcal/mol for D_{2h} B_6S_6 (**1**, 1A_g) at the CCSD(T)//B3LYP level, indicating that the formation of **1** is highly exothermic. To compare the stability of the isomers, the formation energy of D_{3h} B_6S_6 (${}^1A_1'$) (Fig. S1),⁴³ which is similar to the global minimum of $B_3O_3(BO)_3$,¹¹ is also calculated at the same level to be -69.24 kcal/mol. The symmetric D_{2h} structures for $B_6S_6^-$ (**2**) and $B_6S_6^{2-}$ (**3**) also demonstrate the role of B_2S_2 as a robust structural unit.

Interestingly, D_{2h} B_8S_8 (1A_g) (Fig. 3) turns out to be a true minimum with the formation energy of -111.9 kcal/mol with respect to $4B_2S_2$ ($D_{\infty h}$, ${}^1\Sigma_g$) = B_8S_8 (D_{2h} , 1A_g) at the B3LYP level, which can be constructed by combining four distorted linear B_2S_2 units via six S bridges, lending further support for our proposed concept that B_2S_2 is a key structural unit for boron sulfides. We anticipate that this simple structural concept may help design new boron sulfide clusters and nanomaterials.

D. Predicted electronic properties for D_{2h} $B_6S_6^{-/0}$

To aid future experimental studies on D_{2h} B_6S_6 (**1**) and $B_6S_6^-$ (**2**), we predict herein their electronic properties. Ionization potential (IP) is calculated for B_6S_6 (**1**), which amounts to 9.72 eV at the CCSD(T)//B3LYP level. This value is substantially greater than the accurate experimental data for naphthalene (8.135 eV),⁴⁶ suggesting that D_{2h} B_6S_6 (**1**) is a relatively stable species.

Adding one and two extra electrons, respectively, to the non-degenerate LUMO (b_{3u}) of D_{2h} B_6S_6 (**1**), we reach its monoanion $B_6S_6^-$ (**2**) and dianion $B_6S_6^{2-}$ (**3**) with no symmetry distortion (Fig. S4).⁴³ The B—B bond distance within the central B_2 unit shrinks systematically from 1.68 Å in **1**, 1.63 Å in **2**, to 1.61 Å in **3**, indicating that occupation of the b_{3u} CMO strengthens the B—B interaction at the center. We believe the extra electrons in **2** and **3** also promote the formation of an aromatic system in the anion and dianion. Indeed, the bond distances for the bridging B—S units appear to be slightly more even in **3** with respect to **1** (Fig. 1). The ground-state ADE and VDE for $B_6S_6^-$ (**2**) are calculated at B3LYP/6-311+G(d,p) level to be 3.06 and 3.15 eV, respectively.

To facilitate its spectroscopic characterizations, we simulate the photoelectron spectrum of $B_6S_6^-$ (**2**) on the basis of B3LYP/6-311+G(d,p) and TD-DFT^{41,42} data (Fig. 4). The calculated VDEs are listed in Table SII.⁴³ Clearly, there exists a large energy gap of 2.26 eV between the ground-state band (1A_g) and the first excited-state band ($^3B_{3g}$), indicating a remarkably stable neutral cluster, D_{2h} B_6S_6 (**1**). This energy gap serves as characteristic electronic fingerprints for the D_{2h} $B_6S_6^-$ (**2**) and B_6S_6 (**1**) species.

E. $B_6S_6^{-/2-}$ as building blocks in cluster assembled nanomaterials

To assess the potential use of $B_6S_6^-$ (**2**) and $B_6S_6^{2-}$ (**3**) as building blocks for cluster assembled nanomaterials, we have optimized structures of the LiB_6S_6 and $Li_2B_6S_6$ salt complexes, where $B_6S_6^-$ and $B_6S_6^{2-}$ are stabilized by one or two Li^+ counter cations, respectively. Figure 5 shows selected optimized structures of LiB_6S_6 and $Li_2B_6S_6$ at the B3LYP/6-311+G(d,p) level.

Structure LiB_6S_6 (**4**, C_s , $^2A'$) with a perfectly planar B_6S_6 motif is obtained when one Li^+ cation combines with $B_6S_6^-$

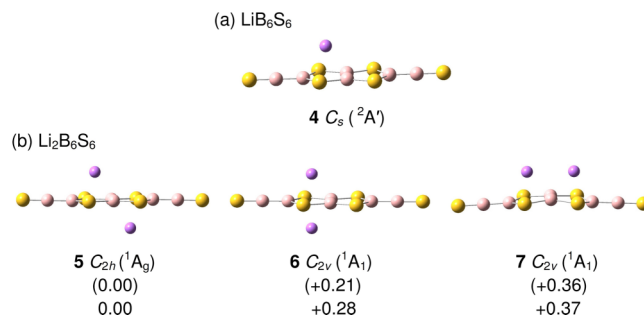


FIG. 5. Optimized structures of LiB_6S_6 (**4**) and $Li_2B_6S_6$ (**5–7**). The relative energies with zero-point energy (ZPE) corrections are shown at the B3LYP/6-311+G(d,p) (in the parentheses) and CCSD(T)//B3LYP/6-311+G(d,p) levels, respectively. All energies are in eV. Yellow color represents S atoms.

(Fig. 5(a)). For $Li_2B_6S_6$, the Li^+ cations approach the dicyclic rings along the fivefold axes, in different combinations, resulting in C_{2h} (**5**, 1A_g), C_{2v} (**6**, 1A_1), and C_{2v} (**7**, 1A_1) complexes (Fig. 5(b)). The C_{2h} $Li_2B_6S_6$ (**5**, 1A_g) complex is the most stable, which lies at least 0.21 and 0.28 eV lower in energy at the B3LYP and CCSD(T)//B3LYP levels, respectively, with respect to the alternative isomers. In C_{2h} $Li_2B_6S_6$ (**5**, 1A_g), the Li^+ cations each coordinate to a B_3S_2 ring, but from opposite sides of the molecular plane. This overall arrangement manages to optimize the electrostatic interactions in the system.

V. CONCLUSIONS

In conclusion, we have presented a series of perfectly planar dicyclic boron sulfide clusters: B_6S_6 (**1**, D_{2h} , 1A_g), $B_6S_6^-$ (**2**, D_{2h} , $^2B_{3u}$), and $B_6S_6^{2-}$ (**3**, D_{2h} , 1A_g). These global-minimum structures are established through extensive global searches and electronic structure calculations at the B3LYP and CCSD(T) levels. The clusters feature twin B_3S_2 five-membered rings as the core with two BS groups attached terminally, in sharp contrast to the lately reported B_6O_6 (D_{3h} , $^1A_1'$) cluster. Chemical bonding analyses reveal a delocalized 10π system for $B_6S_6^{2-}$ (**3**), akin to naphthalene, rendering this dianion a new member of the “inorganic naphthalene” family. To aid their future experimental characterizations, the electronic properties of D_{2h} B_6S_6 (**1**) and $B_6S_6^-$ (**2**) are predicted. A natural question is if we can extend this analogy further to **other boron sulfide systems and design new inorganic analogues of benzene**, anthracene, and other polycyclic aromatic hydrocarbons, which are being actively pursued in our laboratories.

ACKNOWLEDGMENTS

This work was supported by the National Natural Science Foundation of China (21243004 and 21373130), the Research Fund of Binzhou University (2012Y02), and the State Key Laboratory of Quantum Optics and Quantum Optics Devices (KF201402). H.J.Z. gratefully acknowledges the start-up fund from Shanxi University for support.

¹A. P. Sergeeva, D. Y. Zubarev, H. J. Zhai, A. I. Boldyrev, and L. S. Wang, *J. Am. Chem. Soc.* **130**, 7244 (2008).

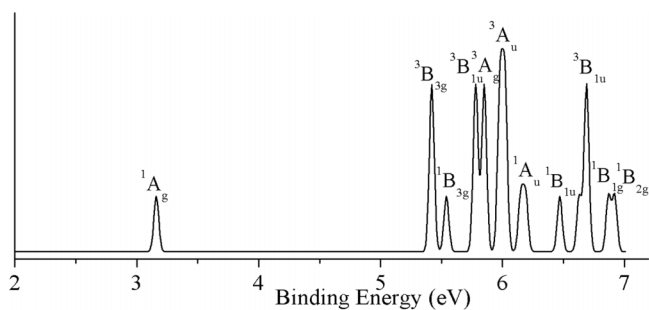


FIG. 4. Simulated photoelectron spectrum of $B_6S_6^-$ (**2**, D_{2h} , $^2B_{3u}$) at the TD-B3LYP/6-311+G(d,p) level. The simulations were done by fitting the distribution of the calculated vertical detachment energies with unit-area Gaussian functions of 0.04 eV half-width.

- ²D. Z. Li, Q. Chen, Y. B. Wu, H. G. Lu, and S. D. Li, *Phys. Chem. Chem. Phys.* **14**, 14769 (2012).
- ³H. J. Zhai, A. N. Alexandrova, K. A. Birch, A. I. Boldyrev, and L. S. Wang, *Angew. Chem., Int. Ed.* **42**, 6004 (2003).
- ⁴H. J. Zhai, B. Kiran, J. Li, and L. S. Wang, *Nat. Mater.* **2**, 827 (2003).
- ⁵J. E. Fowler and J. M. Ugalde, *J. Phys. Chem. A* **104**, 397 (2000); J. Aihara, *ibid.* **105**, 5486 (2001); J. Aihara, H. Kanno, and T. Ishida, *J. Am. Chem. Soc.* **127**, 13324 (2005); A. N. Alexandrova, A. I. Boldyrev, H. J. Zhai, and L. S. Wang, *Coord. Chem. Rev.* **250**, 2811 (2006).
- ⁶A. P. Sergeeva, Z. A. Piazza, C. Romanescu, W. L. Li, A. I. Boldyrev, and L. S. Wang, *J. Am. Chem. Soc.* **134**, 18065 (2012).
- ⁷H. Bai, Q. Chen, C. Q. Miao, Y. W. Mu, Y. B. Wu, H. G. Lu, and H. J. Zhai, *Phys. Chem. Chem. Phys.* **15**, 18872 (2013); H. J. Zhai, Q. Chen, H. Bai, H. G. Lu, W. L. Li, S. D. Li, and L. S. Wang, *J. Chem. Phys.* **139**, 174301 (2013).
- ⁸Q. Chen, H. Bai, J. C. Guo, C. Q. Miao, and S. D. Li, *Phys. Chem. Chem. Phys.* **13**, 20620 (2011); D. Z. Li, H. G. Lu, and S. D. Li, *J. Mol. Model.* **18**, 3161 (2012); Q. Chen and S. D. Li, *J. Cluster Sci.* **22**, 513 (2011).
- ⁹H. J. Zhai, L. S. Wang, A. N. Alexandrova, and A. I. Boldyrev, *J. Chem. Phys.* **117**, 7917 (2002); A. N. Alexandrova, A. I. Boldyrev, H. J. Zhai, L. S. Wang, E. Steiner, and P. W. Fowler, *J. Phys. Chem. A* **107**, 1359 (2003); H. J. Zhai, L. S. Wang, A. N. Alexandrova, A. I. Boldyrev, and V. G. Zakrzewski, *ibid.* **107**, 9319 (2003); A. N. Alexandrova, H. J. Zhai, L. S. Wang, and A. I. Boldyrev, *Inorg. Chem.* **43**, 3552 (2004); A. N. Alexandrova, A. I. Boldyrev, H. J. Zhai, and L. S. Wang, *J. Phys. Chem. A* **108**, 3509 (2004); B. Kiran, S. Bulusu, H. J. Zhai, S. Yoo, X. C. Zeng, and L. S. Wang, *Proc. Natl. Acad. Sci. U. S. A.* **102**, 961 (2005); A. N. Alexandrova, A. I. Boldyrev, H. J. Zhai, and L. S. Wang, *J. Chem. Phys.* **122**, 054313 (2005); W. Huang, A. P. Sergeeva, H. J. Zhai, B. B. Averkiev, L. S. Wang, and A. I. Boldyrev, *Nat. Chem.* **2**, 202 (2010); Q. Chen, G. F. Wei, W. J. Tian, H. Bai, Z. P. Liu, H. J. Zhai, and S. D. Li, *Phys. Chem. Chem. Phys.* **16**, 18282 (2014); W. L. Li, Q. Chen, W. J. Tian, H. Bai, Y. F. Zhao, H. S. Hu, J. Li, H. J. Zhai, S. D. Li, and L. S. Wang, *J. Am. Chem. Soc.* **136**, 12257 (2014).
- ¹⁰H. J. Zhai, Y. F. Zhao, W. L. Li, Q. Chen, H. Bai, H. S. Hu, Z. A. Piazza, W. J. Tian, H. G. Lu, Y. W. Mu, G. F. Wei, Z. P. Liu, J. Li, S. D. Li, and L. S. Wang, *Nat. Chem.* **6**, 727 (2014); H. Bai, Q. Chen, H. J. Zhai, and S. D. Li, "Endohedral and Exohedral Metalloborospherenes: M@B₄₀ (M=Ca, Sr) and M&B₄₀ (M=Be, Mg)," *Angew. Chem., Int. Ed.* (published online).
- ¹¹D. Z. Li, H. Bai, Q. Chen, H. G. Lu, H. J. Zhai, and S. D. Li, *J. Chem. Phys.* **138**, 244304 (2013).
- ¹²D. Z. Li, S. G. Zhang, J. J. Liu, and C. Tang, *Eur. J. Inorg. Chem.* **2014**, 3406.
- ¹³D. Z. Li, C. C. Dong, and S. G. Zhang, *J. Mol. Model.* **19**, 3219 (2013).
- ¹⁴A. Sommer, P. N. Walsh, and D. White, *J. Chem. Phys.* **33**, 296 (1960).
- ¹⁵F. T. Greene and P. W. Gilles, *J. Am. Chem. Soc.* **84**, 3598 (1962).
- ¹⁶F. T. Greene and P. W. Gilles, *J. Am. Chem. Soc.* **86**, 3964 (1964).
- ¹⁷H. Y. Chen and P. W. Gilles, *J. Am. Chem. Soc.* **92**, 2309 (1970).
- ¹⁸H. Y. Chen and P. W. Gilles, *J. Phys. Chem.* **76**, 2035 (1972).
- ¹⁹J. M. Sennegal, J. M. Robbe, and J. Schamps, *Chem. Phys.* **55**, 49 (1981).
- ²⁰P. J. Bruna and F. Grein, *J. Phys. Chem. A* **105**, 3328 (2001).
- ²¹K. P. Huber and G. Herzberg, *Molecular Spectra and Molecular Structure, IV. Constants of Diatomic Molecules* (Van Nostrand, New York, 1979).
- ²²S. G. He, C. J. Evans, and D. J. Clouthier, *J. Chem. Phys.* **119**, 2047 (2003).
- ²³S. G. He and D. J. Clouthier, *J. Chem. Phys.* **120**, 4258 (2004).
- ²⁴Q. L. Guo, J. C. Guo, and S. D. Li, *Chin. J. Struct. Chem.* **27**, 651 (2008).
- ²⁵W. Z. Yao, J. C. Guo, H. G. Lu, and S. D. Li, *J. Phys. Chem. A* **113**, 2561 (2009).
- ²⁶H. J. Zhai, S. D. Li, and L. S. Wang, *J. Am. Chem. Soc.* **129**, 9254 (2007); S. D. Li, H. J. Zhai, and L. S. Wang, *ibid.* **130**, 2573 (2008); H. J. Zhai, L. M. Wang, S. D. Li, and L. S. Wang, *J. Phys. Chem. A* **111**, 1030 (2007); D. Y. Zubarev, A. I. Boldyrev, J. Li, H. J. Zhai, and L. S. Wang, *ibid.* **111**, 1648 (2007); H. J. Zhai, C. Q. Miao, S. D. Li, and L. S. Wang, *ibid.* **114**, 12155 (2010); H. J. Zhai, J. C. Guo, S. D. Li, and L. S. Wang, *ChemPhysChem* **12**, 2549 (2011); Q. Chen, H. J. Zhai, S. D. Li, and L. S. Wang, *J. Chem. Phys.* **137**, 044307 (2012); H. Bai, H. J. Zhai, S. D. Li, and L. S. Wang, *Phys. Chem. Chem. Phys.* **15**, 9646 (2013); Q. Chen, H. Bai, H. J. Zhai, S. D. Li, and L. S. Wang, *J. Chem. Phys.* **139**, 044308 (2013); J. C. Guo, H. G. Lu, H. J. Zhai, and S. D. Li, *J. Phys. Chem. A* **117**, 11587 (2013); W. J. Tian, H. G. Xu, X. Y. Kong, Q. Chen, W. J. Zheng, H. J. Zhai, and S. D. Li, *Phys. Chem. Chem. Phys.* **16**, 5129 (2014); Q. Chen, H. G. Lu, H. J. Zhai, and S. D. Li, *ibid.* **16**, 7274 (2014); H. J. Zhai, Q. Chen, H. Bai, S. D. Li, and L. S. Wang, *Acc. Chem. Res.* **47**, 2435 (2014).
- ²⁷D. Y. Zubarev and A. I. Boldyrev, *Phys. Chem. Chem. Phys.* **10**, 5207 (2008); D. Y. Zubarev and A. I. Boldyrev, *J. Org. Chem.* **73**, 9251 (2008); D. Y. Zubarev and A. I. Boldyrev, *J. Phys. Chem. A* **113**, 866 (2009); T. R. Galeev, Q. Chen, J. C. Guo, H. Bai, C. Q. Miao, H. G. Lu, A. P. Sergeeva, S. D. Li, and A. I. Boldyrev, *Phys. Chem. Chem. Phys.* **13**, 11575 (2011).
- ²⁸A. N. Alexandrova, A. I. Boldyrev, Y. J. Fu, X. Yang, X. B. Wang, and L. S. Wang, *J. Chem. Phys.* **121**, 5709 (2004).
- ²⁹A. N. Alexandrova and A. I. Boldyrev, *J. Chem. Theory Comput.* **1**, 566 (2005).
- ³⁰A. P. Sergeeva, B. B. Averkiev, H. J. Zhai, A. I. Boldyrev, and L. S. Wang, *J. Chem. Phys.* **134**, 224304 (2011).
- ³¹M. Saunders, *J. Comput. Chem.* **25**, 621 (2004); P. P. Bera, K. W. Sattelmeyer, M. Saunders, and P. V. R. Schleyer, *J. Phys. Chem. A* **110**, 4287 (2006).
- ³²D. J. Wales and J. P. K. Doye, *J. Phys. Chem. A* **101**, 5111 (1997).
- ³³A. D. Becke, *J. Chem. Phys.* **98**, 5648 (1993).
- ³⁴C. Lee, W. Yang, and R. G. Parr, *Phys. Rev. B: Condens. Matter Mater. Phys.* **37**, 785 (1988).
- ³⁵M. J. Frisch, G. W. Trucks, H. B. Schlegel, G. E. Scuseria et al., *GAUSSIAN 03, Revision A.01* (Gaussian, Inc., Wallingford, CT, 2004).
- ³⁶J. P. Perdew, K. Burke, and M. Ernzerhof, *Phys. Rev. Lett.* **77**, 3865 (1996).
- ³⁷J. Cizek, *Adv. Chem. Phys.* **14**, 35 (1969).
- ³⁸G. E. Scuseria and H. F. Schaefer III, *J. Chem. Phys.* **90**, 3700 (1989); G. E. Scuseria, C. L. Janssen, and H. F. Schaefer III, *ibid.* **89**, 7382 (1988).
- ³⁹J. A. Pople, M. Head-Gordon, and K. Raghavachari, *J. Chem. Phys.* **87**, 5968 (1987).
- ⁴⁰E. D. Glendening, J. K. Badenhop, A. E. Reed, J. E. Carpenter, J. A. Bohmann, C. M. Morales, and F. Weinhold, *NBO 5.0*, Theoretical Chemistry Institute (University of Wisconsin, Madison, WI, 2001).
- ⁴¹M. E. Casida, C. Jamorski, K. C. Casida, and D. R. Salahub, *J. Chem. Phys.* **108**, 4439 (1998).
- ⁴²R. Bauernschmitt and R. Ahlrichs, *Chem. Phys. Lett.* **256**, 454 (1996).
- ⁴³See supplementary material at <http://dx.doi.org/10.1063/1.4904289> for alternative optimized structures of B₆S₆, B₆S₆⁻, and B₆S₆²⁻; representative optimized structures of B₂S₂; Wiberg bond indices, natural atomic charges, and energy gaps for B₂S₂, B₆S₆ (1), B₆S₆⁻ (2), and B₆S₆²⁻ (3); calculated vertical detachment energies for B₆S₆⁻ (2); and comparison of the π canonical molecular orbitals of B₆S₆^{2-/1-0} (1-3) with those of naphthalene.
- ⁴⁴D. Z. Li and S. D. Li, *J. Mol. Model.* **20**, 2427 (2014).
- ⁴⁵J. R. Soulen and J. L. Margrave, *J. Am. Chem. Soc.* **78**, 2911 (1956).
- ⁴⁶T. Fujiwara and E. C. Lim, *J. Phys. Chem. A* **107**, 4381 (2003).